energies

MDPI

Article

A Comprehensive Inverter-BESS Primary Control for AC Microgrids

Michele Fusero [1], Andrew Tuckey [2], Alessandro Rosini [3,*], Pietro Serra [1], Renato Procopio [3] and Andrea Bonfiglio [3]

1 Grid Edge Solutions ABB S.p.A., 16145 Genova, Italy; michele.fusero@it.abb.com (M.F.); pietro.serra@it.abb.com (P.S.)
2 Grid Edge Solutions ABB Australia Pty Ltd.; andrew.tuckey@au.abb.com
3 Department of Electrical, Electronic, Telecommunication Engineering and Naval Architecture, University of Genoa, 16145 Genova, Italy; renato.procopio@unige.it (R.P.); a.bonfiglio@unige.it (A.B.)
* Correspondence: alessandro.rosini@edu.unige.it

Received: 26 July 2019; Accepted: 1 October 2019; Published: 9 October 2019

Abstract: This paper proposes the design of a comprehensive inverter-BESS primary control capable of providing satisfactory performances both in grid-connected and islanded configurations as required by international standards and grid codes, such as IEEE Std. 1547. Such control guarantees smooth and fast dynamic behavior of the converter in islanded configuration as well as fast power control and voltage-frequency support in grid-connected mode. The performances of the proposed primary control are assessed by means of EMT (ElectroMagnetic Transients) simulations in the dedicated software DIgSILENT PowerFactory® (Germany, Gomaringen) . The simulation results show that the proposed BESS (Battery Energy Storage System) primary control is able to regulate frequency and voltage in Grid-Forming mode independently of the number of paralleled generators. This is achieved adopting a virtual generator technique which presents several advantages compared to the conventional one. Moreover, the proposed control can be switched to Grid-Support mode in order to provide fast control actions to allow frequency and voltage support as well as power control following the reference signals from the secondary level.

Keywords: primary control; BESS; microgrid; Grid Forming; Grid Support; Inverter Control; Grid Support; DIgSILENT PowerFactory; EMT simulations

1. Introduction

The need of pollutant and greenhouse gasses emission reduction and the promising increase of Renewable Energy Sources (RES) have made Microgrids (MG) one of the most interesting and challenging structure for industrial and academic researchers [1]. Several definitions have been provided for a MG but the most effective defines it as a group of interconnected loads and distributed energy resources with clearly defined electrical boundaries that acts as a single controllable entity with respect to the grid and can connect and disconnect from the grid to enable it to operate in both grid-connected or island modes [2]. It is easy to understand that one of the main topics in this field is the control system, and it is well known that it can be structured with a hierarchical structure [3]. Tertiary level control is an energy-production level that must be able to manage the power flow between the MG and the main grid [4]. Secondary level ensures that all the electrical variables into the MG are within the required values and it can include a synchronization control loop to seamlessly connect or disconnect the MG to or from the distribution system [5]. Primary control is typically a communication-less control layer; it is normally implemented in a decentralized manner in order to properly control voltage and frequency and/or active and reactive powers [6]. Finally, inner control

loops are adopted to regulate the output voltage and to control the current while maintaining the system stable. Considering the normative aspect, IEEE Std. 1547 [7] clearly defines the inverter's primary control functionalities that can be essentially clustered in two operational configurations (i) Grid-Following Operation or Grid Support Mode (GSM) and (ii) Grid-Forming Operation. In GSM, the inverter is controlled as a current source in which the main control goals are to supply the load connect to the MG and to participate in frequency and voltage support [8,9]; for these reasons, GSM is the typical configuration in grid-connected state. Grid-Forming Operation is typically exploited in islanded mode where the inverter can be either the voltage and frequency master (stand-alone mode) or allow parallel operations with other Distributed Energy Resources (DERs). An obvious consequence of this high penetration of inverter-interfaced DERs is the reduction of total inertia and damping because most of the proposed control methods for Grid-Forming inverters, e.g., droop control methods [10], provides barely any inertia or damping support for the MG. For this reason, one of the most performing primary control technique for Grid-Forming inverters is the Virtual Synchronous Machine (VSM) or the Virtual Generator Mode (VGM) [11] where the control acts on the inverter in order to mimic the dynamical behavior of a traditional synchronous generator [12–15] virtually adding some inertia and frequency damping to the system and accordingly, improving MG stability and [16], since inertia response is the result of rotating heavy mass and it is proportional to the rotor speed, the VGM concept can also directly improve the frequency response [17]. In [14,18–20], the VGM primary control is developed using the complete model of the synchronous generator and this makes the algorithm complex and the controller tuning difficult. Simpler design models for the VGM control are proposed in [21–24], where only the inertial behavior of a synchronous generator is considered by imposing the swing equation in the primary controller.

In [25], a VGM control technique is proposed showing how it can theoretically provide all the required functionalities of Grid-Forming inverters (according to IEEE Std. 1547) and also presenting some practical applications of VGM control technique for Battery Energy Storage System (BESS) around the world.

Considering all these aspects, the aim of this paper is to present a new primary control for BESS able to guarantee good performances in grid-connected and islanded configurations providing:

- Regulation of frequency and voltage in Grid-Forming mode independently of the number of paralleled generators using the VGM technique in order to mimic the dynamic behavior of synchronous generators;
- Ability to guarantee black-start of the MG in Grid-Forming mode;
- Correct active and reactive power sharing in parallel with other DERs;
- Fast control actions in grid-connected mode to allow providing frequency and voltage support (GSM) as well as power control following the reference signals from the secondary level control;
- Synchronization and connection of the BESS to the external main grid or to other DERs in islanded mode with minimum transients;

The results will show that the new primary control proposed in this paper is also interesting not only from an academic point of view, but also from an industrial one for these aspects:

- The BESS converter is able to work both in VGM and in GSM guaranteeing the possibility to work in parallel with other DERs or an external main grid;
- The primary control can be switched from Grid-Forming mode to Grid-Support mode and vice versa without converter power interruption;
- Considering the Grid-Support mode, the proposed control is able to provide fast actions to the MG because this functionality is implemented in the primary level and not in the secondary one;
- When the support to the MG is not necessary, the control is able to use control signal coming from the secondary level control in order to satisfy other tasks reported in IEEE Std. 1547 such as State of Charge management, power smoothing, and compliance with power flow constraints imposed at the connection point with the external Main Grid (peak lopping);

- Considering the Grid-Forming operating mode, the proposed VGM technique is a PI-based one, which means that the tuning procedure can be easily manged by operators and not just by control engineers.

In summary, all these aspects and the level of detail in which they have been implemented and presented in the paper represent the main contribution of the work and a good starting point for actual implementation on industrial controller (which is the final aim of the ABB/University of Genoa's final goal).

The paper is organized as follows: in Section 2, a description of the BESS primary control is proposed in both the operating configurations. The test case MG implemented in the dedicated power system simulator DIgSILENT PowerFactory® is detailed in Section 3, while simulation results and comments are provided in Section 4. Some conclusive remarks are presented in Section 5.

2. Primary Control Method Description

The aim of this section is to provide an effective description of the proposed primary level BESS control: as stated before, it can provide a correct BESS converter regulation both in Grid-Forming and Grid-Support operating modes as it will be detailed in the following subsections. As one can see from Figure 1, the BESS converter has a R-L-C filter at its output (R_f, L_f and C_f) and the primary control needs some measurements from the field in order to guarantee optimal performances in the two operating modes. In detail, these measurements are active power P_{meas}^{BESS} and reactive power Q_{meas}^{BESS} at the output of the BESS converter, the RMS value of the controlled voltage V_{meas}, the controlled frequency f_{meas} and phase angle θ_{meas} coming from a Phase Locked Loop (PLL) control function synchronized at the connection bus to the MG. The output of the BESS primary control are the reference voltages v_{ref}^{α} and v_{ref}^{β} in the α-β stationary reference frame for the Grid-Forming operating mode and the d-q reference frame currents $i_{d,ref}^{GSM}$ and $i_{q,ref}^{GSM}$ for the Grid-Support operating mode. In order to generate the control signals for the BESS converter $v_{d,ref}^{inv}$ and $v_{q,ref}^{inv}$, voltage and current control loops are mandatory, more precisely when the Grid-Forming operating mode is required, voltage and current control loops are used in a cascade configuration, while in Grid-Support operating mode only the current control loop is required. In the next subsection, VGM and GSM techniques as well as voltage and current control loops are described in detail.

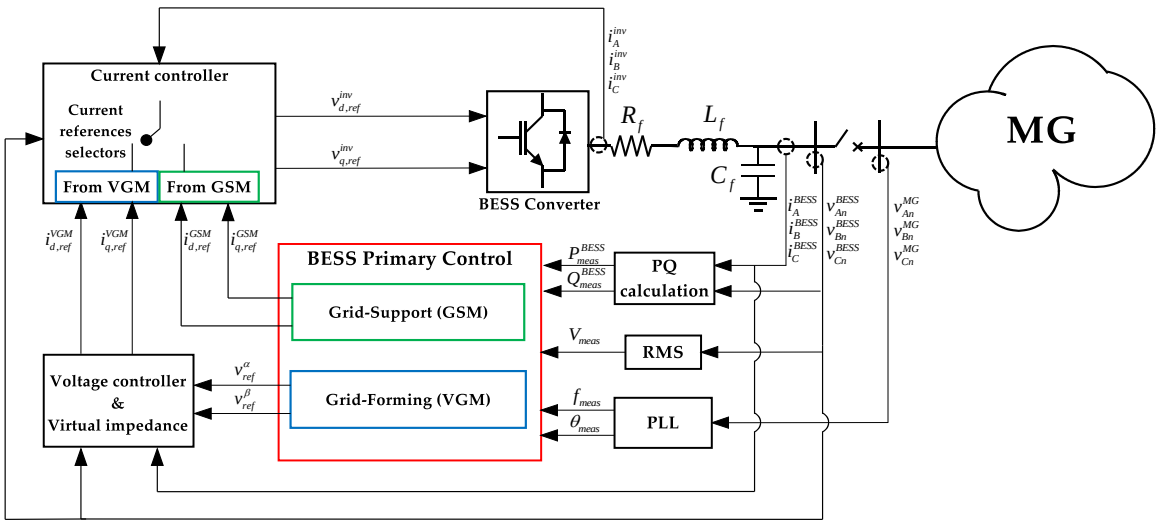

Figure 1. Proposed BESS (Battery Energy Storage System) primary control scheme.

2.1. Grid-Forming Operating Mode: VGM

Considering the Grid-Forming operating mode, the VGM technique presented in [25] is exploited and its control block diagram is reported in Figure 2 where AVR (Automatic Voltage Regulator) and Rotor Flux Model make the reactive power/voltage magnitude similar to that of a synchronous generator. More precisely, the Rotor Flux Model, modeled as an integrator with a gain K_ψ, responds to the reactive power Q_{meas}^{BESS} at the output of the inverter with an initial voltage variation of V_{ref}^{VGM} to model the machine flux variation through the following virtual electrical dynamic equation:

$$\frac{dV_{ref}^{VGM}}{dt} = K_\psi\left(Q_{AVR}^{BESS} - Q_{meas}^{BESS}\right) \tag{1}$$

where Q_{AVR}^{BESS} is the control action of the BESS converter AVR. Then, the AVR brings the RMS voltage at the output of the inverter V_{meas} back to its set point V_{set}. Similarly, the Inertia model and the Frequency Governor make the VGM similar to a synchronous generator active power/frequency dynamics. In particular, the Inertia model, described by an integrator and by two gains K_H for the inertia itself and K_d for the damping effect, reacts to the active power P_{meas}^{BESS} at the output of the inverter, drawing energy from the inertia and slowing the rotational speed of the virtual generator ω_{ref}^{VGM} using the following virtual mechanical dynamic equation:

$$\frac{d\omega_{ref}^{VGM}}{dt} = K_H\left(P_{GOV}^{BESS} - P_{meas}^{BESS} - K_d\omega_{ref}^{VGM}\right) \tag{2}$$

where P_{GOV}^{BESS} is the regulating action of the BESS converter Governor. Then, the Governor brings back the frequency f_{meas} to its set point f_{set}. To allow operation in parallel with other sources, the control includes droop factors m_{droop} and n_{droop} to achieve power sharing control in the steady state; while for stand-alone operation, the droop coefficients are usually set to zero. Then, in order to guarantee the black-start capability [26] of the MG using the BESS, two different selectors are implemented in the control diagram:

- If the measured RMS voltage V_{meas} is zero, the primary control is able to understand the necessity to provide a black-start procedure; so, imposing the logic signal named *Bl-St* equal to 1, the VGM channel is bypassed and the MG is energized using a ramp voltage reference $V_{ref}^{Bl\text{-}St}$ and the rated angular frequency ω_n.
- When the voltage reaches a specific percentage $k_{\%}$ of the rated voltage V_n, the VGM control channel is activated (reset of the control integrators) and the selectors switch to the VGM control actions V_{ref}^{VGM} and θ_{ref}^{VGM}.

Summarizing the above, voltage and frequency references logic for the black-start procedure is:

$$\begin{aligned} &\text{if} \quad 0 \le V_{meas} \le k_{\%}V_n \\ &\qquad Bl-St = 1 \Rightarrow V_{ref} = V_{ref}^{Bl-St} \;\&\; \theta_{ref} = \theta_{ref}^{Bl-St} \\ &\text{if} \quad V_{meas} \ge k_{\%}V_n \\ &\qquad Bl-St = 0 \Rightarrow V_{ref} = V_{ref}^{VGM} \;\&\; \theta_{ref} = \theta_{ref}^{VGM} \end{aligned} \tag{3}$$

Finally, the control actions are transformed in the α-β stationary reference frame.

As a final remark, it is worth pointing out that the tuning procedure of the VGM control is based on a "trial and error" strategy due to the intrinsic simplicity of the proposed primary controller. For example, the inertia parameter K_H of the virtual generator is set in order to have a precise frequency dynamic after an active power step. Then, the governor parameters are set in order to guarantee a desired time response.

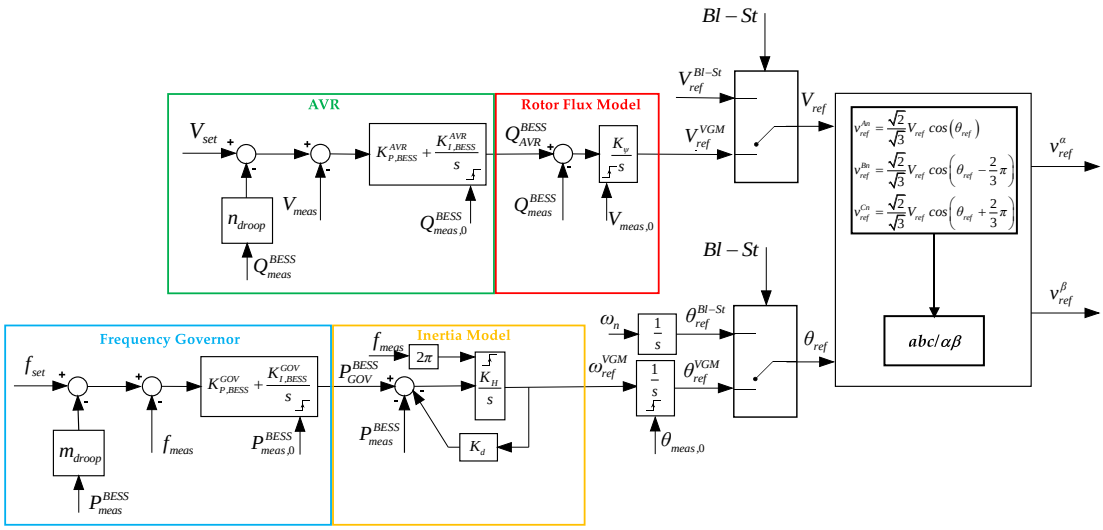

Figure 2. Proposed VGM (Virtual Generator Mode) control model for Grid-Forming operating mode.

2.2. Grid-Support Operating Mode: GSM

Considering now the grid-connected operating mode, the proposed control must provide fast control actions to allow frequency and voltage support (GSM-*fV*) as well as power control following the reference signals from the secondary level control (GSM-*PQ*). To meet these control requests, the block diagram in grid-connected mode is depicted in Figure 3.

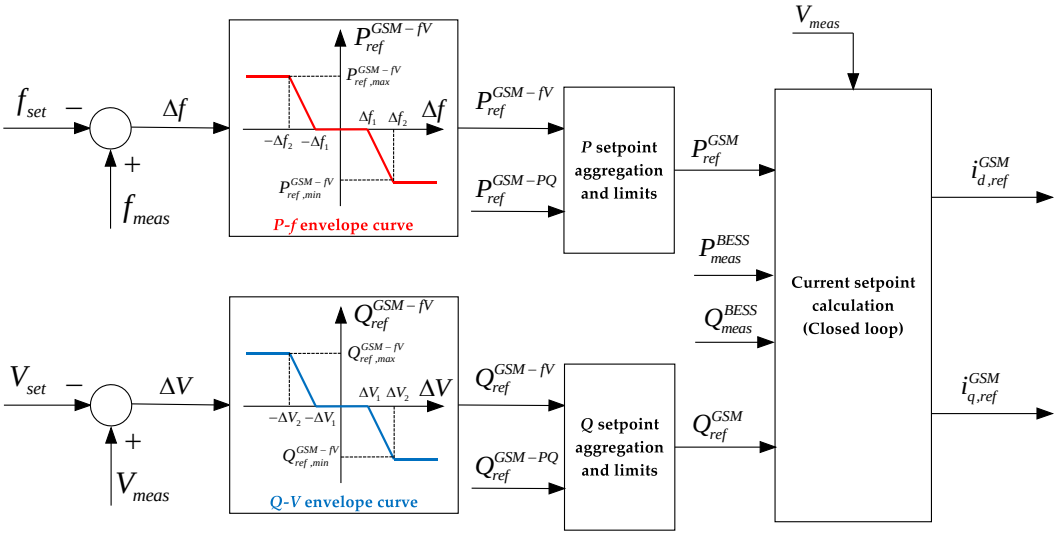

Figure 3. Proposed GSM (Grid Support Mode) control diagram in grid-connected operating mode.

In grid-connected mode, the BESS inverter is controlled starting from the measurements of frequency and voltage at the inverter output, i.e., f_{meas} and V_{meas}, respectively. Based on an error between measurements and respective setpoints, it is possible to carry out the target values of active and reactive powers $P_{ref}^{GSM\text{-fV}}$ and $Q_{ref}^{GSM\text{-fV}}$ through user-defined *P*-*f* envelope curve and *Q*-*V* envelope curve, respectively. Considering, for example, the *P*-*f* envelope curve, it is described by maximum ($P_{ref,max}^{GSM\text{-}PQ}$) and minimum ($P_{ref,min}^{GSM\text{-}PQ}$) active power references and by threshold frequency errors $\pm\Delta f_1$ and $\pm\Delta f_2$. The same characterization is done for the *Q*-*V* envelope curve. As stated before, the control also gives the possibility to track the reference values coming from the secondary level regulation, i.e., $P_{ref}^{GSM\text{-}PQ}$ and $Q_{ref}^{GSM\text{-}PQ}$, so the two blocks "*P* setpoint aggregation and limits" and "*Q* setpoint aggregation

and limits" are implemented. Then, the *d*-*q* axis currents set points $i_{d,ref}^{GSM}$ and $i_{q,ref}^{GSM}$ are generated by closed-loop controllers which use the voltage measurement V_{meas}. Then, they are processed by the BESS inverter Current controller as depicted in Figure 1.

2.3. Voltage and Current Inner Control Loops

In this subsection, the inner control loops of the BESS converter are presented in order to provide a detailed description of the entire control system. Voltage control loop is depicted in Figure 4, and as one can see, it is based on PI regulators described by proportional gain K_{PV} and integral gain K_{IV}. Its main control objective is to regulate the output voltage of the inverter by minimizing the errors between the references $v_{d,ref}^{BESS}$, $v_{q,ref}^{BESS}$ and the measurements v_d^{BESS}, v_q^{BESS}. Moreover, Virtual Impedance strategy is added to the voltage control loop through algebraic manipulation of the α-β voltage reference signals coming from primary controller as follows:

$$v_{ref,v}^{\alpha} = v_{ref}^{\alpha} - \left(R_v i_{\alpha}^{BESS} - X_v i_{\beta}^{BESS}\right) \tag{4}$$

$$v_{ref,v}^{\beta} = v_{ref}^{\beta} - \left(R_v i_{\beta}^{BESS} + X_v i_{\alpha}^{BESS}\right) \tag{5}$$

with R_v and X_v being virtual resistance and reactance, respectively. This modification enables the output impedance to be set (by parameters, or adaptively) and this is usually made predominantly inductive to ensure a strong coupling between active power and frequency, a strong coupling between reactive power and voltage and an inherent decoupling between these two relationships, even in LV microgrids [25]. The outputs of the voltage controller are the inverter output current references $i_{d,ref}^{VGM}$ and $i_{q,ref}^{VGM}$.

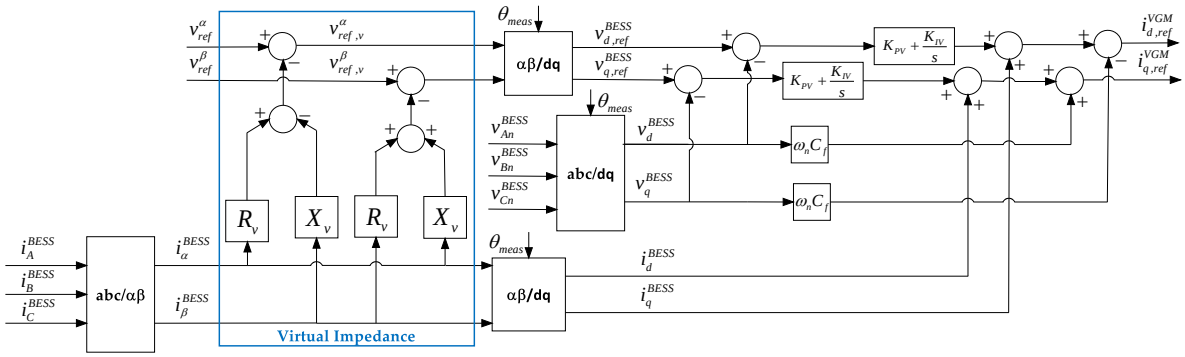

Figure 4. Voltage controller for BESS converter.

Current control loop is instead depicted in Figure 5: due to the fact it is used not only in VGM, but also in GSM operating mode, two selectors are implemented in order to choose the *d*-*q* current references coming from the VGM ($i_{d,ref}^{VGM}$ and $i_{q,ref}^{VGM}$) or from the GSM ($i_{d,ref}^{GSM}$ and $i_{q,ref}^{GSM}$). The current controller is based on PI regulators described by proportional gain K_{PC} and integral gain K_{IC} and it acts on the system in order to control the converter output current by minimizing the errors between the references and the measured current described by i_d^{inv} and i_q^{inv}. The outputs of the current controller are the inverter voltage modulation signals in the *d*-*q* reference frame $v_{d,ref}^{inv}$ and $v_{q,ref}^{inv}$.

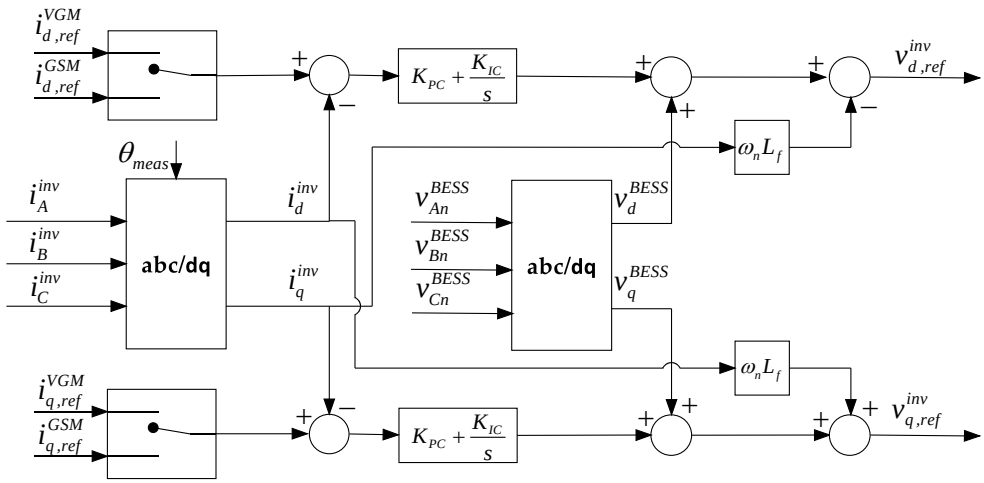

Figure 5. Current controller for BESS converter.

3. DIgSILENT PowerFactory® Model for Testing

3.1. Synchronous Diesel Generator Model for Paralleling Operation

As stated in the introduction section, the proposed BESS control is implemented in the widely used power system simulator DIgSILENT PowerFactory® in order to have reliable and high-fidelity simulation results. Due to the fact that in Grid-Forming operating mode the BESS inverter must be the voltage/frequency master in stand-alone configuration and must allow parallel operations with other DERs, a Synchronous Diesel Generator (SDG) model has been included in the simulated power system; the SDG model is briefly described below starting from the conceptual model depicted in Figure 6.

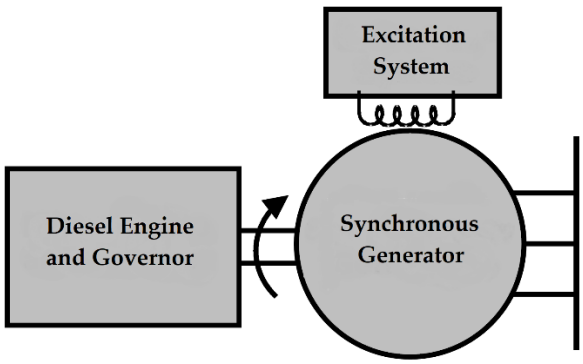

Figure 6. Synchronous Diesel Generator (SDG) conceptual model.

As one can see, it consists of three main elements: Synchronous Generator EMT model is available from PowerFactory library [27], while the Diesel Engine with Governor and Excitation System models are depicted in Figures 7 and 8, respectively.

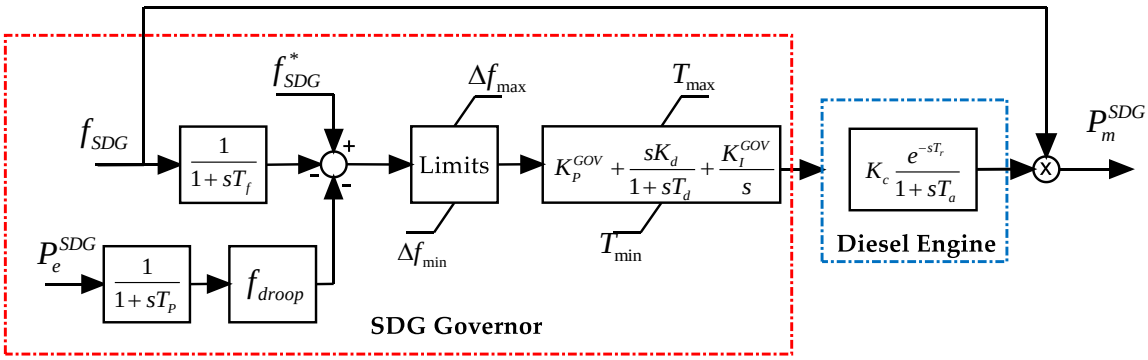

Figure 7. Diesel Engine and Governor model for the SDG.

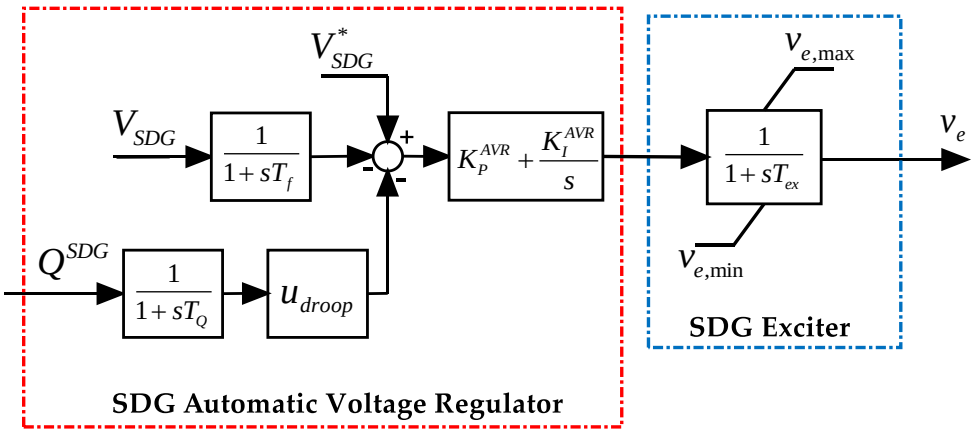

Figure 8. Exciter and Automatic Voltage Regulator model for the SDG.

The frequency-active power regulation of the SDG is realized using a Governor whose inputs are the electrical speed f_{SDG} and the active power measurement P_e^{SDG}. Droop coefficient f_{droop} is implemented to guarantee the correct power sharing in islanded mode and in parallel with the BESS unit. A PID regulator generates the torque input for the diesel generator, which is modeled by the combustion gain K_c, the fuel dynamics time delay T_r, and by a first order dynamic where T_a models the engine fuel system time constant [11]. The voltage-reactive power regulation is performed by an AVR where RMS voltage and reactive power measurements are the inputs and where the droop logic is implemented by the use of the coefficients u_{droop}. The AVR output is then processed by the exciter, which is modeled by a first order dynamic with time constant equal to T_{ex} [28].

3.2. Test MG Layout and Parameters

In order to test the performances of the proposed BESS primary control, the test case MG reported in Figure 9 is used. The main element in the MG is the BESS unit, which is connected to the MG via inverter. The storage component of the BESS is modeled as ideal DC voltage source and so its internal dynamics are neglected. Similarly, the inverter model, provided by DIgSILENT PowerFactory® library, is considered as an ideal controlled AC voltage source. The inverter is interfaced to the MG with a R-L-C filter modeled by the parameters R_f, L_f and C_f, respectively, and with a unitary-ratio transformer T_{BESS}. The SDG exploits the DIgSILENT PowerFactory® synchronous generator model and it is connected to the MG Point of Common Coupling (PCC) using longitudinal impedance $\dot{Z}_{SDG}$. An external grid is connected to the MG through a medium voltage/low voltage transformer $T_{MV\text{-}LV}$ in order to test the Grid support and the paralleling functionalities. Load center bus is connected to the PCC with a line $\dot{Z}_{line}$ while $Load_1$ is connected to Load center bus using a cable $\dot{Z}_{cable}$. MG data are reported in Table 1.

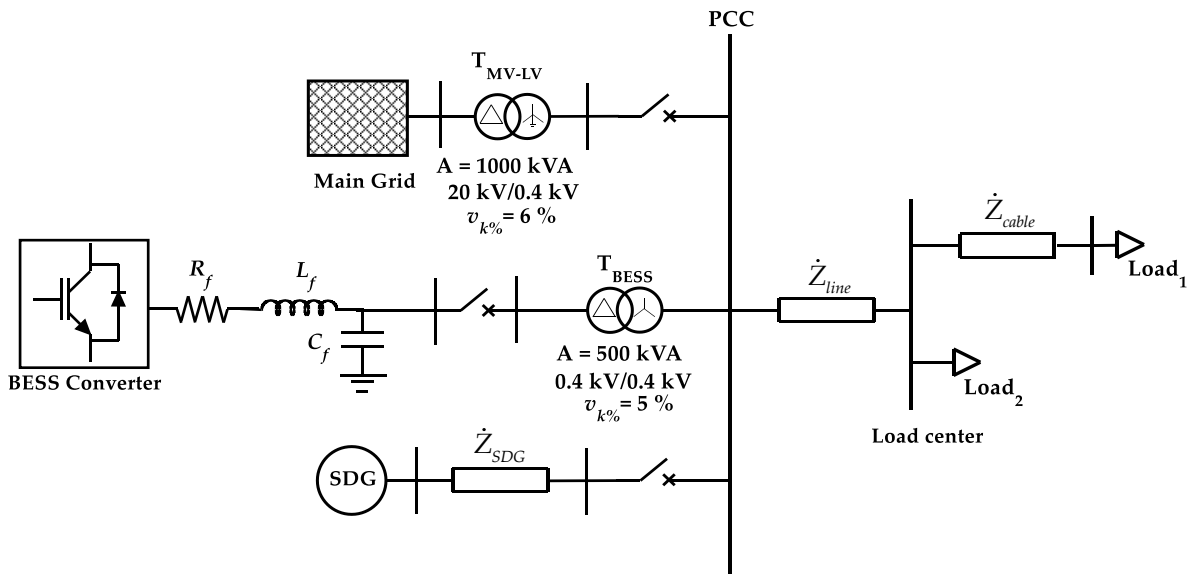

Figure 9. Test case microgrids (MG) one-line diagram.

Table 1. Test case microgrids (MG) parameters.

BESS Converter Data		SDG Data		Load Data		Line and Cables Data at f_n	
A_{BESS}	500 kVA	A_{SDG}	1250 kVA	$P_n(Load_1)$	300 kW	$\dot{Z}_{SDG}$	0.007 + j0.0008 Ω
V_n	400 V (AC-side)	$cos\varphi_n$	0.8	$Q_n(Load_1)$	100 kVAr	$\dot{Z}_{line}$	0.014 + 0.0016 Ω
f_n	50 Hz	V_n	400 V	$P_n(Load_2)$	50 kW	$\dot{Z}_{cable}$	0.0037 + j0.0004 Ω
R_f	0.044 Ω	f_n	50 Hz	$Q_n(Load_2)$	0 kVAr		
L_f	0.088 mH						
C_f	50 μF						

4. Simulations Results

4.1. Black Start and Load Step in a Stand-Alone Configuration

This is the first functionality that the BESS primary control has to satisfy. IEEE 1547.4 Std. gives a clear definition of the black-start, i.e., the ability to start local generation with no external source of power. During this phase, the main grid and the diesel generator are disconnected from the MG and no load is connected. As described in the previous section, the BESS is controlled in Grid-Forming operating mode and the VGM control is bypassed imposing voltage and frequency reference signals. As one can see from Figure 10, the three-phase voltages at the controlled node of the MG perfectly follow the ramp reference signal V_{ref}, and the zoomed box highlights the correct dynamic behavior when the VGM control channel is activated with the switch of V_{ref} from $V_{ref}^{Bl\text{-}St}$ to V_{ref}^{VGM} and of θ_{ref} from $\theta_{ref}^{Bl\text{-}St}$ to θ_{ref}^{VGM} and with the reset of the integrators of the VGM control.

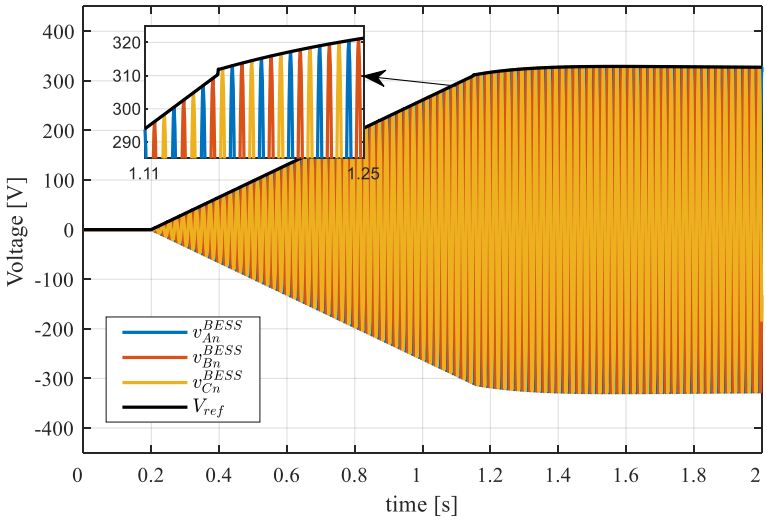

Figure 10. Controlled BESS bus voltage time profiles during black-start procedure.

When the black-start procedure ends (the ramping time is defined through a parameter and in this case it was chosen to last 1 s), a load step event is implemented in the simulation in order to test the dynamic response of the BESS in VGM mode in terms of voltage and frequency in a stand-alone configuration. As one can see from Figure 11, after the load step occurred at t = 4 s, frequency and voltage have a time profile in which it is possible to note the effects of the inertia model and of the governor regulating action for the frequency and of rotor flux model and AVR regulating action for the voltage. In this simulation, the droop coefficient m_{droop} and n_{droop} are equal to zero because the power sharing functionality is not required in a stand-alone configuration, and for this reason, after the transient, frequency and voltage return to their rated values (namely 50 Hz for the frequency and 400 V for the voltage). Moreover, it is possible to notice the effect of the virtual impedance implemented in the voltage control loop of the converter; in fact, in the final steady state, the reference value V_{ref}^{VGM} is greater than the controlled inverter output voltage V_{meas}. Finally, Figure 12 reports the active and reactive powers' time profile after load step contingency (P_{load} and Q_{load}), and it is possible to see how the BESS is able to supply the load power request with a fast and smooth dynamic response.

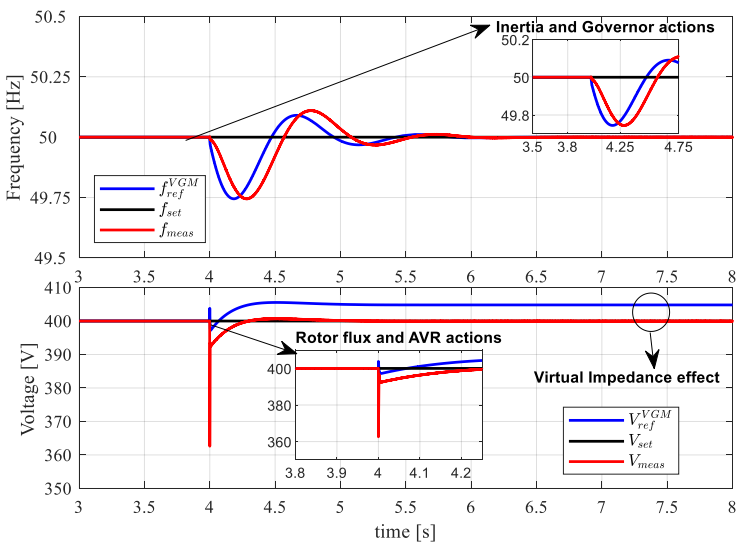

Figure 11. Frequencies (first panel) and RMS (Root Mean Square) voltages (second panel) time profile during load step in stand-alone configuration.

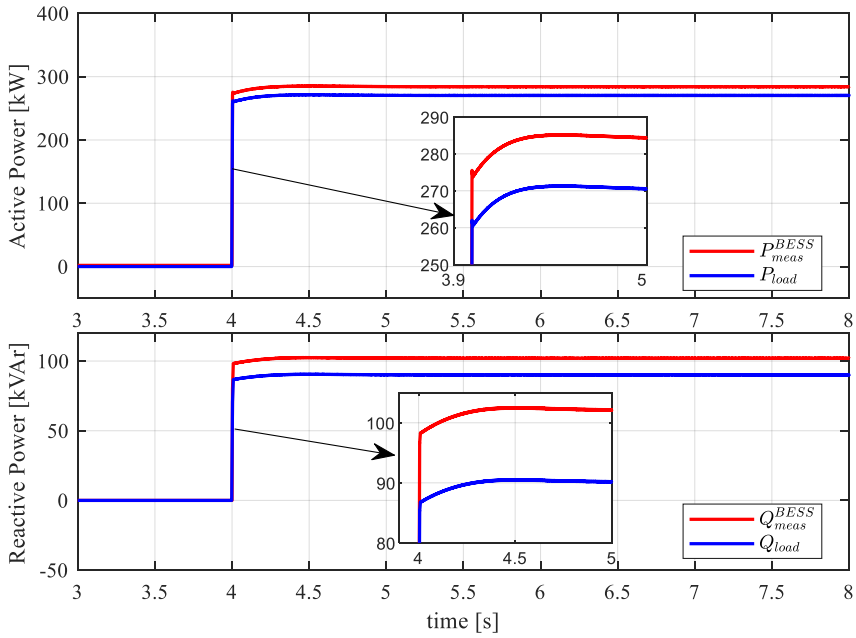

Figure 12. Active (first panel) and reactive (second panel) powers' time profile during load step in stand-alone configuration.

4.2. VGM Operating Mode With Setpoints Variation

As stated in the introduction, when the VGM operating mode is activated, the BESS converter has to provide fast regulation of voltage and frequency. In these simulations, the main grid is connected to the MG and the load request is totally fed by the main grid. The BESS converter is then connected to the MG in Grid-Forming operating mode without active and reactive powers production. In order to highlight the advantages of the proposed VGM control technique, a comparison with the conventional droop control for Grid-Forming operating mode is proposed. When this conventional control technique is adopted, all the macro blocks of the proposed controller (i.e., the AVR, the Rotor Flux Model, the Governor and the Inertia Model) are bypassed avoiding all the dynamics introduced by the virtual generator scheme. So, the control signals V_{ref} and θ_{ref} with the conventional droop control technique become:

$$\begin{cases} V_{ref} = V_{set} - n_{droop} Q_{meas}^{BESS} \\ \theta_{ref} = 2\pi \int_0^t \left[f_{set}(s) - m_{droop} P_{meas}^{BESS}(s) \right] ds \end{cases} \tag{6}$$

The first simulation results are depicted in Figure 13: in this scenario, the frequency setpoint f_{set} is fixed at the MG rated value, while the voltage setpoint V_{set} changes from 400 V to 410 V at t = 2 s, then from 410 V to 390 V at t = 6 s and finally from 390 V to 400 V at t = 10 s. As one can see, the set point is correctly followed by the controlled RMS voltage V_{meas} with good time response and minimum overshoots (the droop parameters m_{droop} and n_{droop} are equal to zero in this simulation since there are no other DERs to share the load request). The second panel shows instead reactive powers time profile, and it is possible to see that an increase/decrease of the controlled voltage corresponds to a BESS converter reactive power production/absorption, which is balanced by the main grid, due to the strong coupling between voltage and reactive power. Considering the comparison, the conventional droop control has a faster time response because there is no effect of the virtual generator dynamics, but it has two main drawbacks: (i) voltage steady-state errors due to the absence of an AVR in the droop control to compensate the effect of the virtual impedance implemented in the voltage controller (the greater the output current of the BESS converter, the greater the voltage steady-state error, as apparent in Equations (4) and (5)) and (ii) large initial overshoots in the reactive power time profiles as detailed in Figure 14.

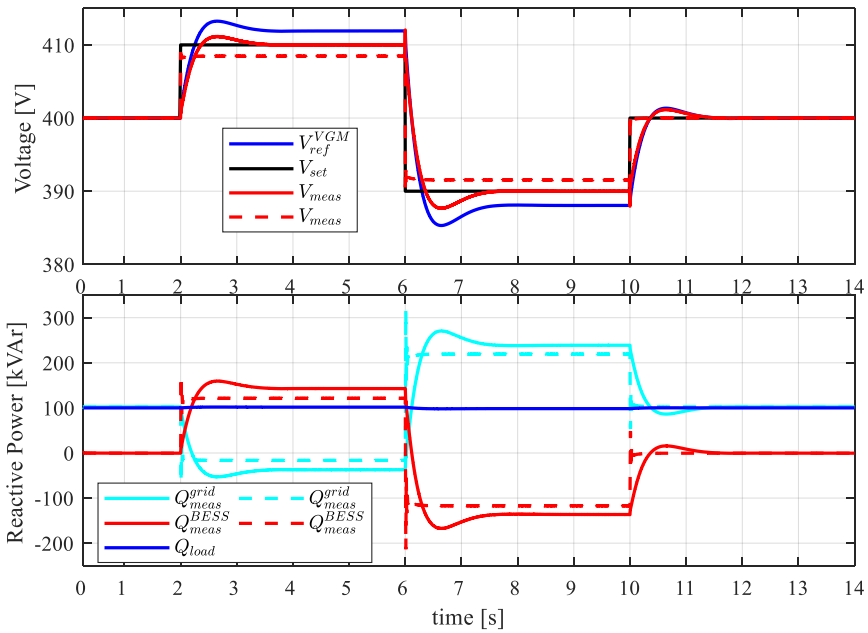

Figure 13. Voltage (first panel) and reactive powers (second panel) time profiles with voltage setpoint variations with Virtual Generator Mode (VGM) (solid lines) and conventional (dotted lines) techniques.

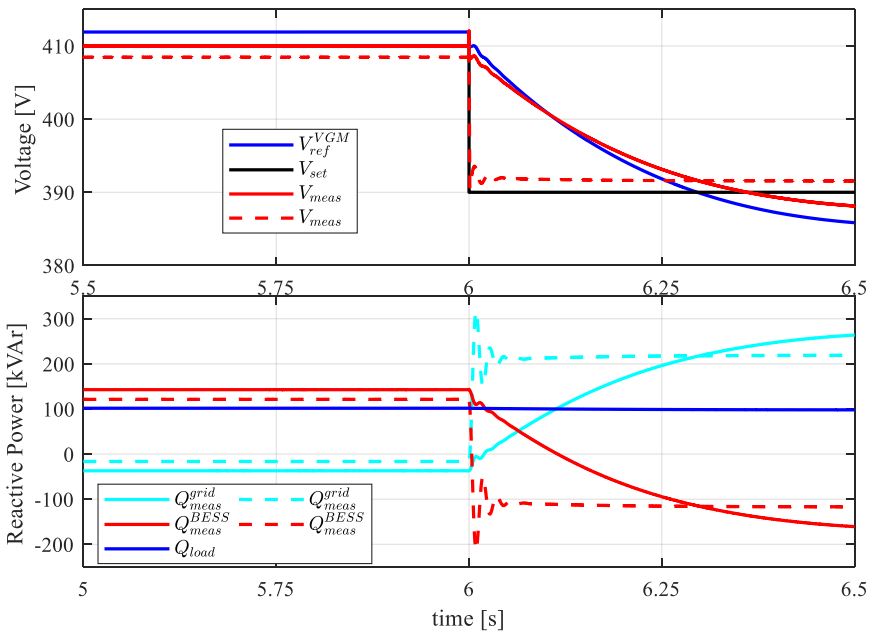

Figure 14. Detail on the comparison between the proposed technique (solid lines) and conventional droop control (dotted lines).

Then, in order to test the possibility of managing the BESS converter active power production by changing the frequency setpoint, in the second scenario the voltage setpoint V_{set} is fixed to the rated value while the frequency setpoint f_{set} changes from 50 Hz to 50.1 Hz V at t = 2 s, then from 50.1 Hz to 49.9 Hz V at t = 6 s and finally from 49.9 Hz to 50 Hz at t = 10 s. Due to synchronism with Main Grid requirement, the frequency droop factor m_{droop} is activated. As one can see from Figure 15, the frequency setpoint is not tracked (first panel), but varying its value it is possible to correctly manage the BESS active power production (second panel), which is correctly balanced by the Main Grid. Also, in this test case, conventional droop control guarantees a faster active power regulation due to the

lack of the virtual inertia of the VGM control technique but, as one can see from Figure 16, the droop control creates a greater frequency variation in the very first transient.

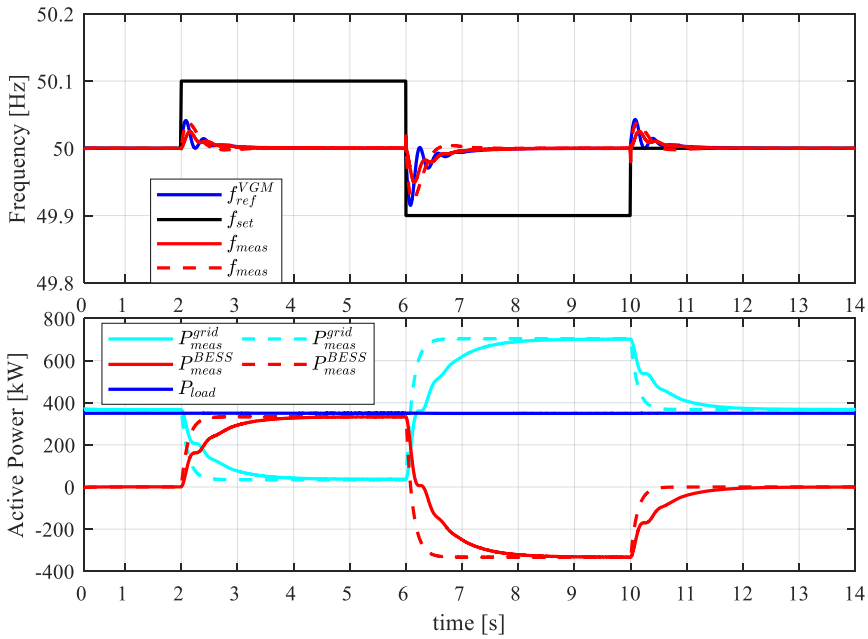

Figure 15. Frequency (first panel) and active powers (second panel) time profiles with frequency setpoint variations with VGM (solid lines) and conventional (dotted lines) techniques.

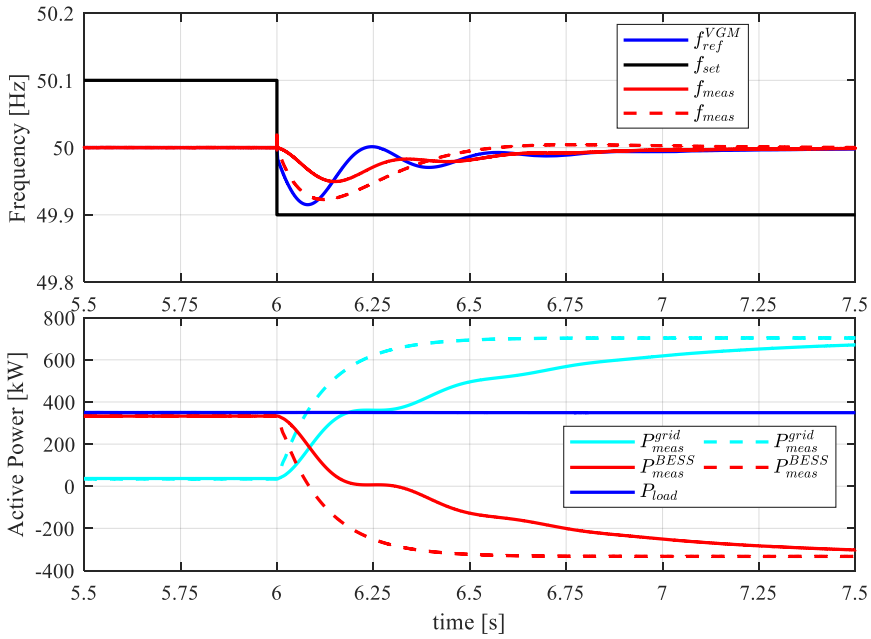

Figure 16. Detail on the comparison between the proposed technique (solid lines) and conventional droop control (dotted lines).

4.3. Paralleling Action and Load Sharing

The aim of this simulation is to show how the BESS converter can be connected to an islanded MG where a diesel generator is already online in Grid-Forming operating mode and to also show the correct power sharing functionality. As one can see from Figure 17, at t = 0.1 s a live-start of the BESS converter is activated: as one can see, the controlled voltage (v_{AN}^{BESS}, v_{BN}^{BESS}, v_{CN}^{BESS}) starts to

follow the connection bus voltages (v_{AN}^{MG}, v_{BN}^{MG}, v_{CN}^{MG}) and, at t = 0.2 s, the phase reference output of the primary control θ_{ref}^{VGM} is synchronized with the measured phase angle θ_{meas} at the connection bus to the MG. Finally, at t = 0.25 s, the AC-breaker of the BESS converter is closed and in Figure 18 is possible to notice a really limited power transient quantifiable in a transient current less than 1% of the BESS-converter-rated value current.

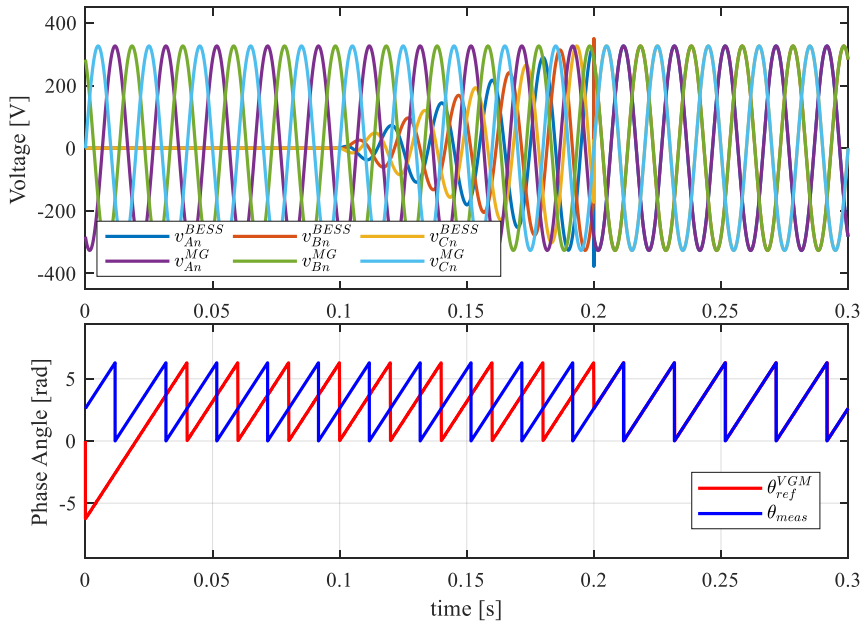

Figure 17. Voltage (first panel) and phase angles (second panel) during synchronization with MG.

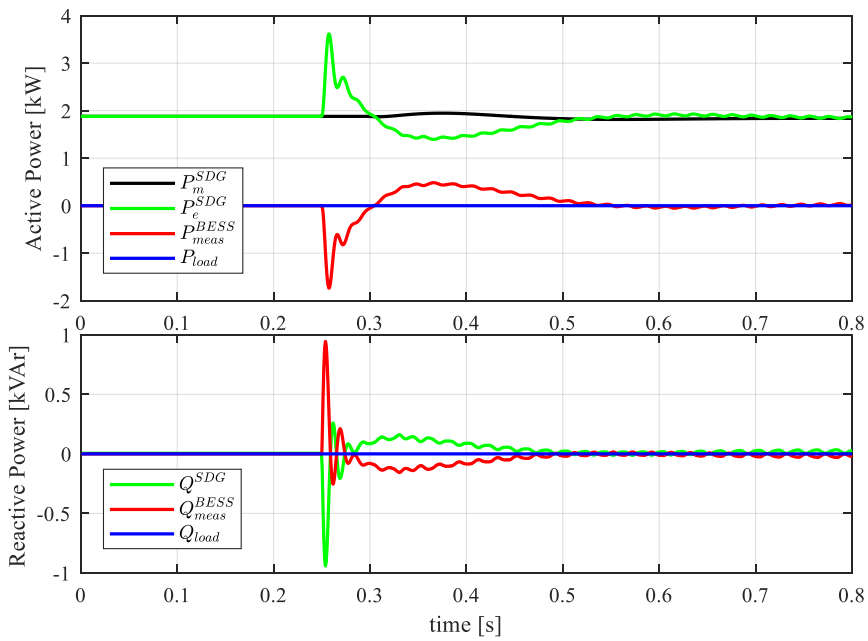

Figure 18. Active (first panel) and reactive (second panel) powers time profile during paralleling procedure.

Then in order to test the proper active and reactive power sharing between the diesel generator and the BESS, a load step contingency is implemented at t = 4 s. Figure 19 shows active and reactive powers time profile and it is possible to highlight the correct active and reactive power sharing according to the rated apparent power of the two units. The proper active power sharing can be guaranteed by the relation $A_{BESS} m_{droop} = A_{SDG} f_{droop}$, while a correct reactive power sharing can be achieved if the droop

factors n_{droop} for the BESS and u_{droop} for the diesel generator are correctly set in order to overcome the mismatch in the connection impedances to the MG of the two units. The virtual impedance $R_v + jX_v$ affects the reactive power sharing only during the transient, because in steady state its effect is nulled out by the BESS AVR regulating action on the controlled voltage V_{meas}. Instead, Figure 20 shows frequencies and RMS voltages time profile during the load step contingency and it is possible to highlight the inertial behavior of the BESS converter and voltage and frequency deviations from the respective rated values according to the droop logic in the proposed primary control.

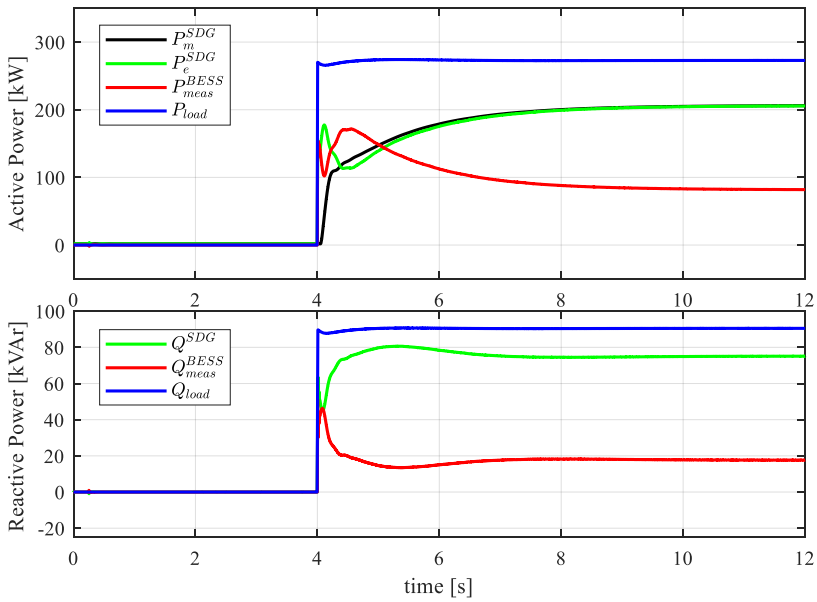

Figure 19. Active (first panel) and reactive (second panel) powers time during load step in paralleling configuration.

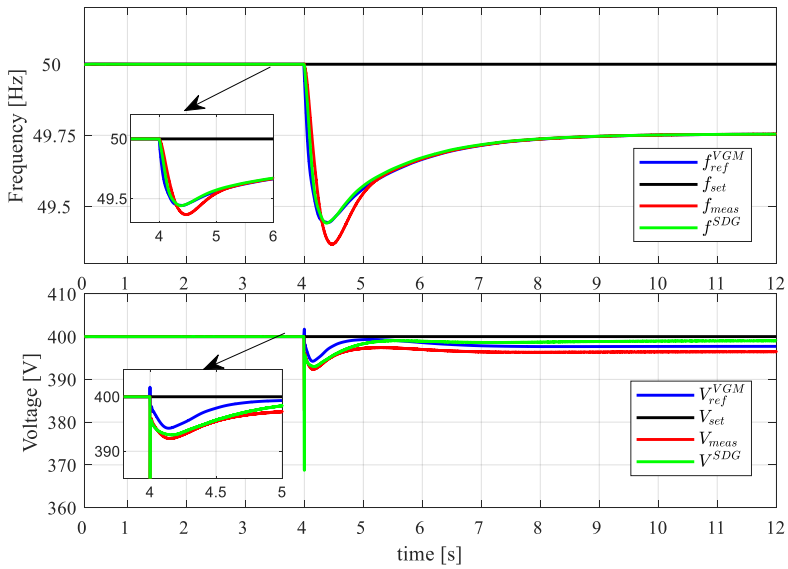

Figure 20. Frequencies (first panel) and RMS voltages (second panel) time profile in paralleling configuration.

4.4. Grid Support Action

In this subsection, the results of the BESS converter controlled in GSM operating mode are presented in detail. The first simulation is carried out in order to test the correct behavior of the proposed primary control in GSM-*fV*, i.e., when the active/reactive power references come from the envelope curves. In order to highlight the positive effects of the BESS converter in support mode, two different MG configurations are considered:

- In the first configuration, the BESS converter is not connected to the MG. Two different loads, namely Load_1 and Load_2, are connected to the MG with $P_{load,1} = 300$ kW, $Q_{load,1} = 100$ kVAr and $P_{load,2} = 50$ kW (pure resistive load). Loads are supplied by the SDG, while the main grid is disconnected.
- In the second configuration, the BESS is connected to the MG in GSM-*fV* mode ready to provide voltage and frequency support after MG contingencies.

At $t = 2$ s, Load_1 is disconnected to the MG and simulation results are depicted in Figures 21 and 22.

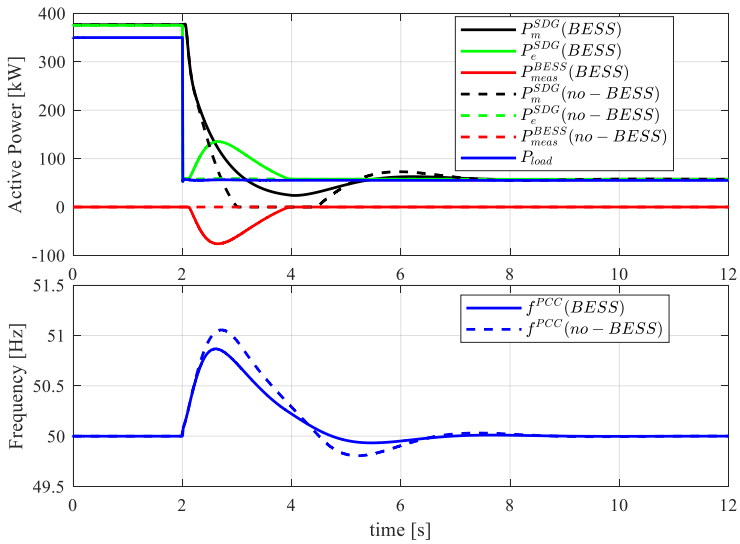

Figure 21. Active powers and Point of Common Coupling (PCC) frequency in Grid Support Mode (GSM)-*fV* mode.

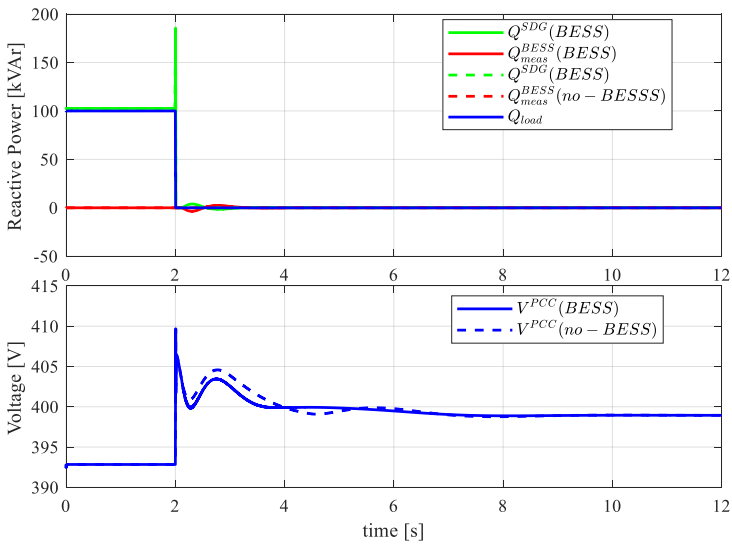

Figure 22. Reactive powers and PCC voltage in GSM-*fV* mode.

As one can see after the load disconnection, MG frequency f^{PCC} and voltage V^{PCC} (measured at PCC) start to increase: if the BESS is connected in GSM mode, when voltage and frequency exceed the threshold values Δf_1 and ΔV_1, respectively, the BESS converter starts to absorb active and reactive power according the implemented envelope curves. It is easy to notice that the dynamic response in terms of frequency and voltage with BESS converter controlled in GSM-*fV* mode (solid lines) is better with respect to the response without BESS connected to the MG (dashed lines). Finally, Figure 23 shows the correct response of the primary controller in GSM-*PQ* mode, i.e., when the active and reactive power references $P_{ref}^{GSM\text{-}PQ}$ and $Q_{ref}^{GSM\text{-}PQ}$ are not provided by envelope curve, but are sent by the system controller. In this configuration, the SDG is not connected, while the MG is connected to the main grid: the primary controller is able to correctly track powers references guaranteeing fast regulating actions.

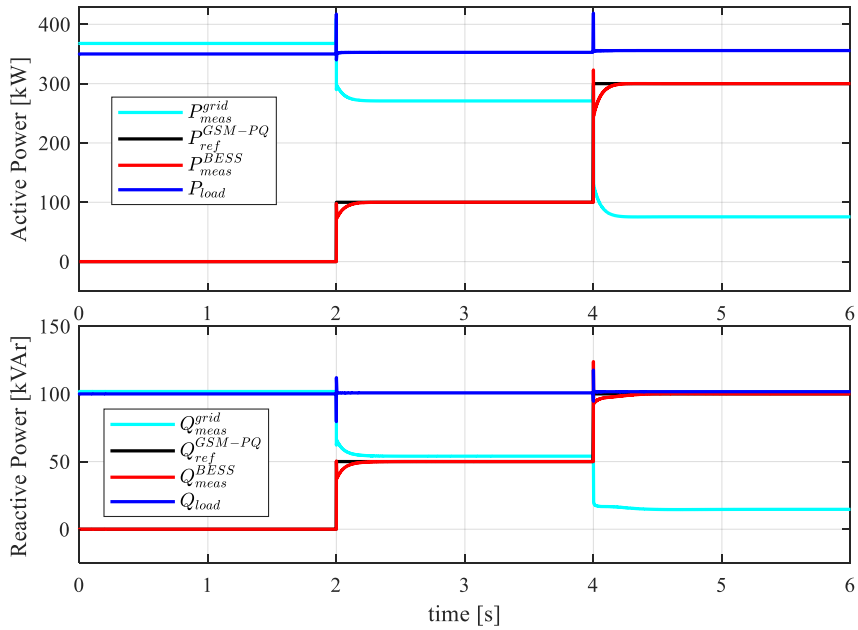

Figure 23. Active and reactive powers time profile in GSM-PQ mode.

5. Conclusions

This paper proposed a comprehensive primary control for BESS converter in order to provide all the regulations required by IEEE Std. 1547 both in grid-connected and islanded configurations. Due to the need to guarantee fast and smooth dynamics of voltage and frequency in islanded configuration, the BESS converter is controlled using a VGM technique in order to have it acting on the system as a real synchronous generator. Simulations are carried out using the dedicated simulation software DIgSILENT PowerFactory® and show that the proposed controller is able to provide the black-start capability, to regulate frequency and voltage independently of the number of paralleled generators, to synchronize and connect BESS converter to the external main grid or to other DERs in with minimum transients and to guarantee a proper active/reactive power sharing among other DERs. Moreover, simulations showed that the proposed primary control has the possibility to provide fast control actions also in grid-connected mode to allow providing frequency and voltage support (GSM-fV) as well as power control following the reference signals from the secondary level control (GSM-PQ). Future works will be focused on the transitions between the two operating modes in order to provide system stability during planned or unplanned islanding or during the reconnection of the main grid.

Author Contributions: M.F., A.T. and A.R. designed the Primary Regulator, A.R. performed the simulations and wrote the paper. P.S., R.P. and A.B. provided supervision to the research activity, provided critical analysis to the results achieved by simulations and revised the manuscript.

Funding: This research received no external funding.

Conflicts of Interest: The authors declare no conflict of interest.

References

1. Mariam, L.; Basu, M.; Conlon, M.F. Microgrid: Architecture, policy and future trends. *Renew. Sustain. Energy Rev.* **2016**, *64*, 477–489. [CrossRef]
2. U.S.D.O. Energy. *DOE Microgrid Workshop Report*. Available online: https://www.energy.gov/about-us (accessed on 27 October 2018).
3. Guerrero, J.M.; Vasquez, J.C.; Matas, J.; de Vicuña, L.G.; Castilla, M. Hierarchical control of droop-controlled AC and DC microgrids—A general approach toward standardization. *IEEE Trans. Ind. Electron.* **2011**, *58*, 158–172. [CrossRef]
4. Luna, A.C.; Meng, L.; Diaz, N.L.; Graells, M.; Vasquez, J.C.; Guerrero, J.M. Online Energy Management Systems for Microgrids: Experimental Validation and Assessment Framework. *IEEE Trans. Power Electron.* **2018**, *33*, 2201–2215. [CrossRef]
5. Lu, X.; Yu, X.; Lai, J.; Wang, Y.; Guerrero, J.M. A Novel Distributed Secondary Coordination Control Approach for Islanded Microgrids. *IEEE Trans. Smart Grid* **2018**, *9*, 2726–2740. [CrossRef]
6. Bidram, A.; Davoudi, A. Hierarchical Structure of Microgrids Control System. *IEEE Trans. Smart Grid* **2012**, *3*, 1963–1976. [CrossRef]
7. IEEE PES Industry Technical Support Task Force. *Impact of IEEE 1547 Standard on Smart Inverters*; Technical Report PES-TR67; IEEE: Piscataway, NJ, USA, 2018.
8. Zeineldin, H.H. A*Q*–*f*Droop Curve for Facilitating Islanding Detection of Inverter-Based Distributed Generation. *IEEE Trans. Power Electron.* **2009**, *24*, 665–673. [CrossRef]
9. Zeineldin, H.H.; El-saadany, E.F.; Salama, M.M.A. Distributed Generation Micro-Grid Operation: Control and Protection. In Proceedings of the 2006 Power Systems Conference: Advanced Metering, Protection, Control, Communication, and Distributed Resources, Clemson, SC, USA, 14–17 March 2006; pp. 105–111.
10. Liu, J.; Miura, Y.; Ise, T. Comparison of Dynamic Characteristics Between Virtual Synchronous Generator and Droop Control in Inverter-Based Distributed Generators. *IEEE Trans. Power Electron.* **2016**, *31*, 3600–3611. [CrossRef]
11. Bevrani, H. *Robust Power System Frequency Control*; Springer: Berlin/Heidelberg, Germany, 2009; Volume 85.
12. Rocabert, J.; Luna, A.; Blaabjerg, F.; Rodriguez, P. Control of power converters in AC microgrids. *IEEE Trans. Power Electron.* **2012**, *27*, 4734–4749. [CrossRef]
13. Zhong, Q.; Weiss, G. Synchronverters: Inverters That Mimic Synchronous Generators. *IEEE Trans. Ind. Electron.* **2011**, *58*, 1259–1267. [CrossRef]
14. Zhong, Q.; Nguyen, P.; Ma, Z.; Sheng, W. Self-Synchronized Synchronverters: Inverters Without a Dedicated Synchronization Unit. *IEEE Trans. Power Electron.* **2014**, *29*, 617–630. [CrossRef]
15. Zhong, Q.; Konstantopoulos, G.C.; Ren, B.; Krstic, M. Improved Synchronverters with Bounded Frequency and Voltage for Smart Grid Integration. *IEEE Trans. Smart Grid* **2018**, *9*, 786–796. [CrossRef]
16. Arco, S.D.; Suul, J.A. Virtual synchronous machines—Classification of implementations and analysis of equivalence to droop controllers for microgrids. In Proceedings of the 2013 IEEE Grenoble Conference, Grenoble, France, 16–20 June 2013; pp. 1–7.
17. Fathi, A.; Shafiee, Q.; Bevrani, H. Robust Frequency Control of Microgrids Using an Extended Virtual Synchronous Generator. *IEEE Trans. Power Syst.* **2018**, *33*, 6289–6297. [CrossRef]
18. Hirase, Y.; Noro, O.; Yoshimura, E.; Nakagawa, H.; Sakimoto, K.; Shindo, Y. Virtual synchronous generator control with double decoupled synchronous reference frame for single-phase inverter. *IEEJ J. Ind. Appl.* **2015**, *4*, 143–151. [CrossRef]
19. Chen, Y.; Hesse, R.; Turschner, D.; Beck, H. Improving the grid power quality using virtual synchronous machines. In Proceedings of the 2011 International Conference on Power Engineering, Energy and Electrical Drives, Torremolinos, Spain, 11–13 May 2011; pp. 1–6.
20. Xiang-zhen, Y.; Jian-hui, S.; Ming, D.; Jin-wei, L.; Yan, D. Control strategy for virtual synchronous generator in microgrid. In Proceedings of the 2011 4th International Conference on Electric Utility Deregulation and Restructuring and Power Technologies (DRPT), Weihai, Shandong, China, 6–9 July 2011; pp. 1633–1637.

21. Sakimoto, K.; Miura, Y.; Ise, T. Stabilization of a power system with a distributed generator by a Virtual Synchronous Generator function. In Proceedings of the 8th International Conference on Power Electronics—ECCE Asia, Jeju, Korea, 29 May–2 June 2011; pp. 1498–1505.
22. Shintai, T.; Miura, Y.; Ise, T. Reactive power control for load sharing with virtual synchronous generator control. In Proceedings of the 7th International Power Electronics and Motion Control Conference, Harbin, China, 2–5 Jun 2012; pp. 846–853.
23. Shintai, T.; Miura, Y.; Ise, T. Oscillation Damping of a Distributed Generator Using a Virtual Synchronous Generator. *IEEE Trans. Power Deliv.* **2014**, *29*, 668–676. [CrossRef]
24. Alipoor, J.; Miura, Y.; Ise, T. Power System Stabilization Using Virtual Synchronous Generator With Alternating Moment of Inertia. *IEEE J. Emerg. Sel. Top. Power Electron.* **2015**, *3*, 451–458. [CrossRef]
25. Tuckey, A.; Round, S. Practical application of a complete virtual synchronous generator control method for microgrid and grid-edge applications. In Proceedings of the 2018 IEEE 19th Workshop on Control and Modeling for Power Electronics (COMPEL), Padova, Italy, 25–28 June 2018; pp. 1–6.
26. Lopes, J.P.; Moreira, C.; Resende, F. Control strategies for microgrids black start and islanded operation. *Int. J. Distrib. Energy Resour.* **2005**, *1*, 241–261.
27. D. GmbH. *DIgSILENT PowerFactory 2017 User Manual*; DIgSILENT: Gomaringen, Germany, 2017.
28. Kundur, P.; Balu, N.J.; Lauby, M.G. *Power System Stability and Control*; McGraw-Hill: New York, NY, USA, 1994; Volume 7.

© 2019 by the authors. Licensee MDPI, Basel, Switzerland. This article is an open access article distributed under the terms and conditions of the Creative Commons Attribution (CC BY) license (http://creativecommons.org/licenses/by/4.0/).